Nucleated Antiparallel β-Sheet That Folds and Undergoes Self-Assembly: A Template Promoted Folding Strategy toward Controlled Molecular Architectures

Danny W. Choo, Joel P. Schneider, Nilsa R. Graciani, and Jeffery W. Kelly*

Department of Chemistry, Texas A&M University, College Station, Texas 77843-3255

Received May 23, 1995; Revised Manuscript Received September 22, 1995[⊗]

ABSTRACT: The aromatic amino acid residue 4-(2-aminoethyl)-6-dibenzofuranpropanoic acid (**1**) nucleates antiparallel β-sheet folding in tridecapeptides which subsequently self-assemble into fibrils. Residue **1** functions as a folding nucleator by facilitating intramolecular hydrogen bonding between the flanking α-amino acid residues and by favoring the formation of a hydrophobic cluster composed of the dibenzofuran skeleton and the hydrophobic side chains of the flanking α-amino acids. The hydrogen bonded hydrophobic cluster (i.e., −hydrophobic α-amino acid residue−**1**−hydrophobic α-amino acid residue−) nucleates β-sheet folding in relatively small peptides that have a propensity to fold. The α-amino acid sequence design determines the self-association pathway and the resulting molecular architecture. The approach described here takes advantage of template driven hydrophobic clusters and template derived conformational biases to nucleate folding in small peptides, affording β-sheets which subsequently self-associate into well-defined quaternary structures. This strategy allows significant α-amino acid sequence variations to be accommodated in the resulting β-sheet-based macromolecular assembly without interfering with the folding pathway.

Our understanding of β-sheet structure lags significantly behind our understanding of α-helical secondary structure due, in part, to the lack of a well-defined peptide model system for studies on β-sheet structure.[1] Careful studies on peptide model systems have significantly improved our mechanistic understanding of helical folding.[2] However, it has proven much more difficult to design a peptide that will fold into a monomeric β-sheet in aqueous solution.[3] Small peptides having a predominance of β-branched residues typically undergo self-association in addition to intramolecular folding, affording heterogeneous aggregated β-sheet structures characterized by a mixture of parallel and antiparallel β-strand orientations, with a few exceptions.[3] High molecular weight polypeptides composed of a single residue or a repeating dipeptide sequence having a propensity to adopt a β-sheet structure also form heterogeneous β-sheets.[4] In an effort to nucleate the folding of a structurally well-defined β-sheet, we have reported a dibenzofuran-based amino acid residue, namely, 4-(2-aminoethyl)-6-dibenzofuranpropanoic acid (**1**). This template reverses the polypeptide chain direction by replacing the $i + 1$ and $i + 2$ residues of a β-turn and facilitates strand−strand interactions in appropriate sequences resulting in β-sheet formation.[5]

Variable temperature NMR analysis, FT-IR studies, and X-ray crystallographic data demonstrate that residue **1** promotes intramolecular hydrogen bonding between the flanking α-amino acid residues, which appears to be necessary but not sufficient for nucleating β-sheet folding in the attached peptide strands.[5] Residue **1** can adopt two different conformations in aqueous solution, as discerned by X-ray crystallographic and 2D-NMR studies, both having the attached α-amino acids intramolecularly hydrogen bonded. The nucleation competent conformation places the dibenzofuran ring perpendicular to the plane of the amide−amide intramolecular hydrogen bonds defining the β-sheet, Figure 1. The perpendicular conformation of **1** is stabilized by hydrophobic interactions between the dibenzofuran skeleton and the hydrophobic side chains of the α-amino acid residues that flank **1**, resulting in the formation of a hydrophobic cluster.[5a] Hence, it is the hydrogen bonded hydrophobic cluster afforded by the sequence −hydrophobic residue−**1**−hydrophobic residue− that is responsible for β-sheet nucleation. Sequences such as V-K-L-**1**-V-K-L-NH_2 adopt a monomeric β-sheet-like structure in the portion of the molecule which is proximal to **1**; however, heptapeptides incorporating **1** do not fold cooperatively, nor do they adopt a well-defined structure toward the N- and C-termini.[5a,d] In an effort to create cooperatively folded, well-defined β-sheet structures, we used longer α-amino

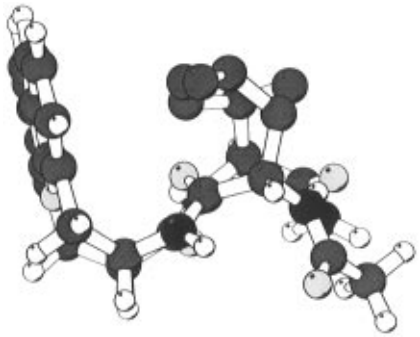

Figure 1. Molecular Graphics depiction[27] of Ac-Leu-**1**-Val-NH_2, demonstrating the perpendicular conformation that residue **1** can adopt in aqueous solution. Although residue **1** can also exist in a more extended conformation in nonpolar solvents, it is the perpendicular conformation which supports the hydrophobic cluster in aqueous solution. The hydrophobic cluster conformation is stabilized by hydrophobic interactions between the dibenzofuran skeleton and the side chains of the flanking α-amino acid residues, as established by NOESY-NMR and near-UV CD studies.[5a] The view shown positions the dibenzofuran skeleton and the intramolecular hydrogen bonds perpendicular to the plane of the page (H's have been deleted from the α-amino acid side chains for clarity).

[⊗] Abstract published in *Advance ACS Abstracts,* November 15, 1995.

0024-9297/96/2229-0355$12.00/0

Table 1

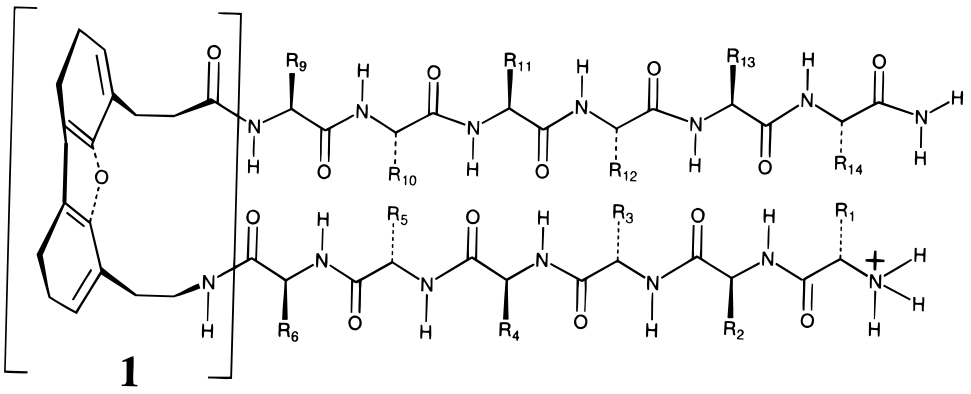

1

peptide	R1	R2	R3	R4	R5	R6	R7	R8	R9	R10	R11	R12	R13	R14
A	Lys	Val	Lys	Val	Lys	Val	**-1-**		Val	Lys	Val	Lys	Val	Lys
B	*N-AcLys*	Val	Lys	Val	Lys	Val	**-1-**		Val	Lys	Val	Lys	Val	Lys
C	Lys	Val	*Lys·Tfa*	Val	Lys	Val	**-1-**		Val	Lys	Val	Lys	Val	Lys
D	Lys	Val	Lys	Val	*Lys·Tfa*	Val	**-1-**		Val	Lys	Val	Lys	Val	Lys
E	Lys	Val	Lys	Val	Lys	Val	**-1-**		Val	*Lys·Tfa*	Val	Lys	Val	Lys
F	Lys	Val	Lys	Val	Lys	Val	**-1-**		Val	Lys	Val	*Lys·Tfa*	Val	Lys
G	Lys	Val	*Lys·Tfa*	Val	Lys	Val	**-1-**		Val	Lys	Val	*Lys·Tfa*	Val	Lys
H	Lys	Val	Lys	Val	*Lys·Tfa*	Val	**-1-**		Val	*Lys·Tfa*	Val	Lys	Val	Lys
I	Lys	Val	*Lys·Tfa*	Val	Lys	Val	**-1-**		Val	*Lys·Tfa*	Val	Lys	Val	Lys
J	Lys	Val	Lys	Val	*Lys·Tfa*	Val	**-1-**		Val	Lys	Val	*Lys·Tfa*	Val	Lys
K	Lys	Val	Lys	Val	Lys	Val	*Gly-Gly*		Val	Lys	Val	Lys	Val	Lys
L	Lys	Val	Lys	Val	Lys	Val	*D-Phe-Pro*		Val	Lys	Val	Lys	Val	Lys
M	Val	Lys	Val	Lys	Val	Lys	**-1-**		Lys	Val	Lys	Val	Lys	Val

acid sequences incorporating **1**. We have recently discovered tridecapeptide sequences that undergo intramolecular folding affording monomeric well-defined β-sheet model systems[6] and sequences that undergo intramolecular folding and subsequently self-associate into β-sheet quaternary structures. The work described within focuses on tridecapeptides incorporating **1** which undergo intramolecular antiparallel β-sheet folding and β-sheet mediated self-assembly, affording a soluble β-sheet fibril. This study demonstrates the potential of template-promoted folding in the preparation of macromolecular architectures in aqueous solution.[7]

Tridecapeptides based on the sequence K-V-K-V-K-V-**1**-V-K-V-K-V-K-NH_2 were prepared because sequential polypeptides of the type $(Lys\text{-}Val)_n$, where n is > 25, are known to undergo a coil to self-associated β-sheet transition upon titration from acidic pH to pH 8.8 in the absence of added salt.[4b] A slow coil to β-sheet transition was also observed in the case of poly$(Lys\text{-}Val)_n$ at pH 2.3 upon addition of 100 mM NaCl. In both cases these β-sheets form by extensive self-association and are heterogeneous. The $(Lys\text{-}Val)_n$ rich tridecapeptide **A** incorporating residue **1** has been designed such that upon intramolecular folding a monomeric amphiphilic β-sheet structure is afforded. The exposed hydrophobic surface of the amphiphilic sheet should self-associate due to the hydrophobic effect producing a dimeric face to face β-sheet sandwich.[8] Under appropriate conditions the dimeric β-sheet sandwich was expected to self-associate via intermolecular β-sheet formation into a high-MW quaternary structure.

Naturally occurring fibrous proteins such as silks are composed mainly of repetitive amino acid sequences having a high degree of β-sheet structure in addition to amorphous domains.[9] It has been proposed that the remarkable mechanical properties (i.e., high tensile strength, excellent extensibility, and lateral resiliency) of these fibrous proteins arise, at least in part, from the tertiary and quaternary β-sheet structure.[9] Because of the potential applications of silk-like fibrils in materials science, many researchers have strived to mimic their physical properties.[10] Silk mimics have been synthesized either by chemical methods or employment of bacterial overexpression systems.[10] Difficulties encountered in the folding of these polypeptides has hampered progress in the preparation of silk mimics. One potentially reliable approach for obtaining predictable folding is to incorporate templates into predominantly α-amino acid sequences. The potential advantages of such an approach are that substantial α-amino acid sequence variation can be tolerated without interfering with the folding pathway because the template is the major folding influence. In addition, small sequences could be utilized if the intramolecularly folded sequences are designed to self-assemble via intermolecular β-sheet formation to make macromolecular assemblies. To demonstrate the validity of this concept, the amino acid residue **1** was incorporated into the K-V rich tridecapeptide (peptide **A**) to nucleate intramolecular antiparallel β-sheet folding. The folded β-sheet structure subsequently self-assembles into fibrils having a β-sheet quaternary structure.[11] Extensions of this approach to sheets that associate into lamellar architectures like those found in silk are ongoing and will be reported in due course.

Results and Discussion

Effect of Charge(s) on the Folding of Peptide A. Several tridecapeptides composed of repeating -Lys-Val- sequences and analogues thereof have been synthesized using a standard Merrifield solid phase strategy. Tridecapeptide **A** having the -Lys-Val- rich sequence shown in Table 1 has an overall charge of +7 at low pH. In acidic buffers the high positive charge density of the sequence surrounding **1** prevents the strands from interacting to form an intramolecular β-sheet structure, explaining the random coil behavior of peptide **A** at low pH, Figure 2. Removal of charge(s) from peptide **A** by

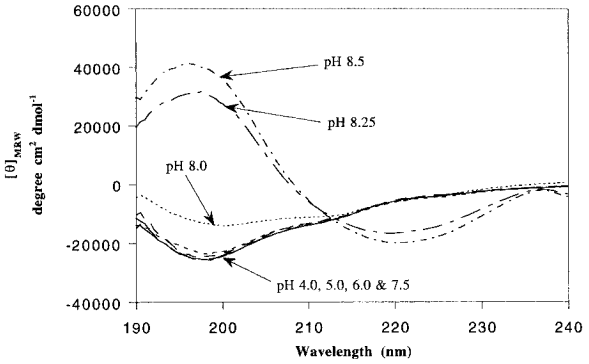

Figure 2. Far-UV CD spectra of 0.1 mM peptide **A** as a function of pH.

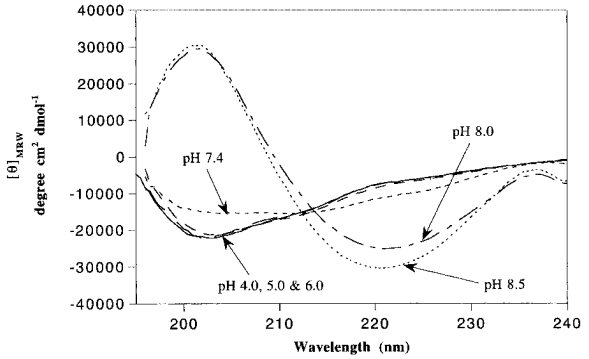

Figure 3. Far-UV CD spectra of 0.1 mM peptide **B** as a function of pH.

increasing the pH to 8.5 appears to be sufficient to effect a coil to β-sheet transition (Figure 2).

A series of peptides were prepared and studied to identify the charges which require neutralization for folding to occur in peptide **A**. Although the N-terminal amino group is expected to have the lowest pK_a (7.8) of all the ammonium groups in peptide **A**, the N-terminally acetylated analogue of peptide **A**, peptide **B**, exhibits a pH dependent coil to β-sheet transition that is similar to that of peptide **A**, indicating that the removal of this charge is not sufficient for initiating the coil to sheet transition observed in peptide **A** at pH 8.5 (Figure 3). Therefore, it appears that one or more of the charges on the Lys side chain ϵ-ammonium groups is being neutralized at pH 8.5 in peptide **A**, allowing β-sheet folding to occur. Given the polycationic nature of peptide **A**, it is reasonable to expect that the pK_a values of the side chain ammonium groups would be lowered significantly from the normal value of 10.4. Peptides **C**−**F** were prepared to determine whether the neutralization of one ϵ-ammonium group was sufficient to achieve folding in peptide **A** (Table 1). The importance of a given ammonium group(s) in the folding of peptide **A** was probed by converting that group to a trifluoroacetamide, which is uncharged. The subset of peptides that exhibit pH independent β-sheet folding serve to identify the specific Lys residue(s) whose neutralization allows peptide **A** to fold into a β-sheet structure. Peptides **C**−**F** exhibit pH dependent coil to sheet folding transitions, Figure 4, indicating that the neutralization of one ϵ-ammonium group was insufficient to allow folding in peptide **A** at low pH.

The bis(trifluoroacetylated) peptides **G**−**J** were prepared to determine if the removal of two charges in peptide **A** would be sufficient to facilitate pH independent β-sheet folding (Table 1). Peptide **G** was prepared first because it was anticipated that the side chain ammonium groups of Lys-3 and Lys-12 in peptide **A** would have the lowest pK_a values as these should experience the highest charge repulsion in the folded β-sheet. Peptide **G**, having both Lys-3 and Lys-12 N^{ϵ}-trifluoroacetylated, adopts a pH independent β-sheet structure over the pH range of 4−8.5 in 75 mM NaCl, indicating that the removal of both of these charges in peptide **A** is sufficient to allow folding (Figure 5) at low pH.[12] Bis(trifluoroacetylated) peptide **H**, having both Lys-5 and Lys-10 N^{ϵ}-trifluoroacetylated, exhibits an analogous pH independent β-sheet structure, suggesting that removal of this pair of charges is also sufficient to allow for β-sheet folding in peptide **A**.[13] The fact that peptides **G** and **H** both fold in a pH independent fashion suggests that the removal of two charges is sufficient to initiate folding in peptide **A**. From these studies it is not discernible which pair of charged Lys residues are neutralized in peptide **A** at pH 8.5. In fact, it could be that nonspecific removal of two Lys side chain charges is sufficient to allow for folding in peptide **A**. Bis(trifluoroacetylated) peptides **I** and **J** were prepared to test this possibility (Table 1). Interestingly, as in the case of peptides **G** and **H**, both peptides **I** and **J** adopt a β-sheet conformation at pH 4 (75 mM NaCl) as determined by far-UV CD studies.[13] It appears that removal of two of the Lys side chain charges from the four possible Lys residues 3, 5, 10, and 12 in peptide **A** is sufficient to allow for strand collapse, affording a β-sheet structure nucleated by hydrophobic residue−**1**−hydrophobic residue. It is not surprising that several different pairwise deprotonations of the Lys side chains would have similar effects on folding owing to the flexibility of the Lys side chains and the ability of the remaining ammonium groups to reorient themselves so as to be as far apart as possible. These studies conclusively demonstrate that removal of two charges is necessary for folding to occur, however, it is not possible to specify which two Lys side chain charges in peptide **A** are neutralized at pH 8.5.

The β-sheet folding transition facilitated by neutralizing two of the Lys side chain charges in peptide **A** should also be achievable at low pH if sufficient salt is added to shield unfavorable charge−charge interactions.[14] The effectiveness of a series of monovalent salts was measured by the minimal concentration required to produce the coil to β-sheet structural transition in peptide **A** at pH 4.0, as discerned by far-UV CD. This study indicates that $NaClO_4$ is more effective than NaCl, which is more effective than NaF, at inducing β-sheet formation, Figure 6. The order of effectiveness of the anions ($ClO_4^- > Cl^- > F^-$) is consistent with the electroselectivity series and can be interpreted as being due to the electroselectivity of the anion for binding to and neutralizing the positively charged ammonium groups in peptide **A**.[15] Multivalent anions such as PO_4^{3-} and SO_4^{2-} were also evaluated for their ability to induce a sheet structure in peptide **A** at pH 4.0. These anions cause peptide **A** to precipitate from solution consistent with very tight binding to the ammonium groups of Lys, facilitating folding[14,15] and self-association leading to an insoluble β-sheet quaternary structure due to the neutralization of charge. The order of anion effectiveness is opposite to that expected if a Hofmeister effect was responsible for the coil to sheet transition ($F^- > Cl^- > ClO_4^-$).[16] The Hofmeister effect (solvent effect) generally requires high salt concentrations, well above those used here.

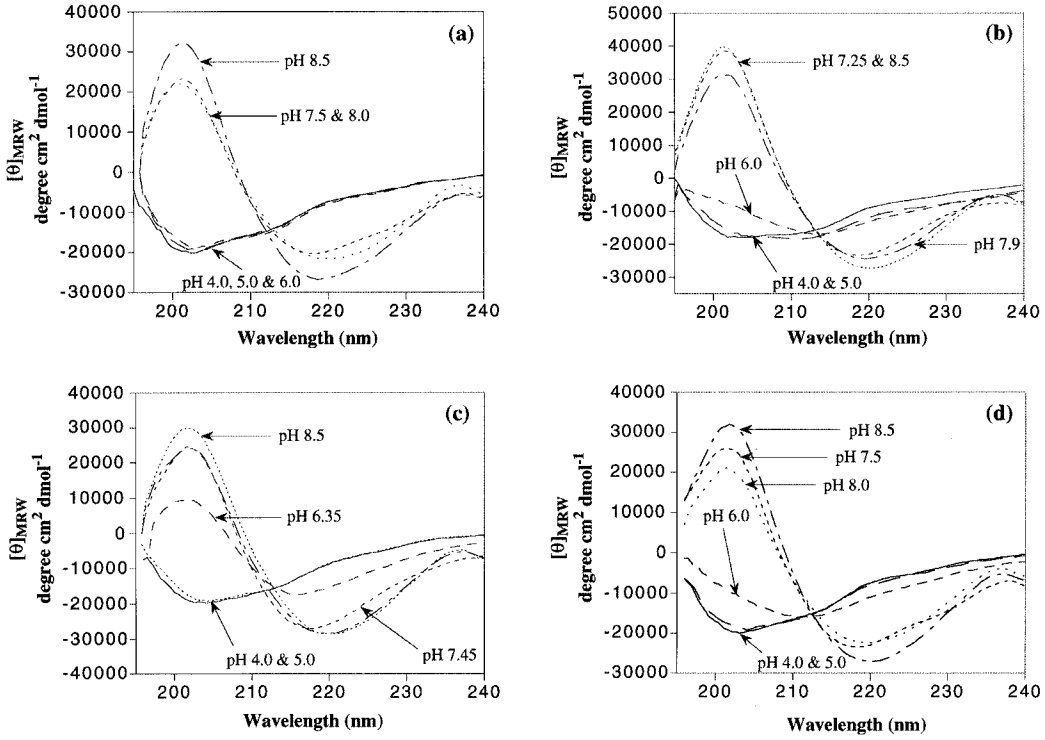

Figure 4. Far-UV CD spectra of 0.1 mM (a) peptide **C**, (b) peptide **D**, (c) peptide **E**, and (d) peptide **F** as a function of pH.

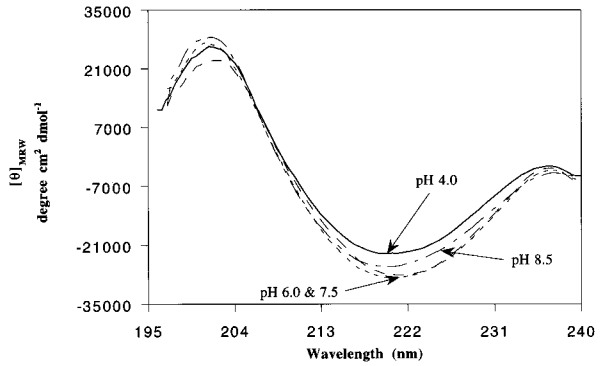

Figure 5. Far-UV CD spectra of 0.1 mM peptide **G** in 75 mM NaCl as a function of pH.

Importance of the Hydrophobic Cluster in Nucleating *β*-Sheet Structure. It is expected that the sequence -Val-**1**-Val- adopts a hydrogen bonded hydrophobic cluster conformation which is poised and waiting to nucleate folding once solution conditions permit strand−strand interactions. Peptides **K**−**M** were synthesized in order to evaluate the importance of residue **1** in the folding of peptide **A** (Table 1). Peptide **K** has the same amphiphilic α-amino acid sequence as that of peptide **A**, except that the nucleator **1** is replaced with the dipeptide sequence Gly−Gly. Replacement of **1** with the dipeptide Gly−Gly should allow this portion of peptide **K** the flexibility to sample a number of possible conformations, including a reverse turn conformation, and to fold into a *β*-sheet structure if the K-V-based α-amino acid sequence has a propensity to do so. Peptide **K** is not competent to fold into a *β*-sheet structure at pH 8.5 (Figure 7a), suggesting that both the nucleator **1** and the amphiphilic sequence are required for *β*-sheet folding. In order to further demonstrate the importance of residue **1** in the folding of peptide **A**, a consensus $i + 1$, $i + 2$ type II′ *β*-turn sequence (D-Phe-Pro) was substituted for **1** in peptide **A** to generate peptide **L**. The D-Phe-Pro sequence optimizes the likelihood of chain reversal and folding if the K-V sequence in peptide **L** has the propensity to do so. Peptide **L** is not capable of folding at pH 8.5, strongly suggesting that both **1** and the amphiphilic sequence in peptide **A** together are responsible for its folding at pH 8.5, Figure 7b.

Peptide **M** was synthesized to probe the importance of the hydrophobic cluster, -Val-**1**-Val-, in the folding of peptide **A**. Peptide **M** has the same amino acid composition as peptide **A** and maintains a hydrophobic periodicity of 2, but differs in sequence. In peptide **M**, Lys residues flank **1** instead of the Val residues which surround **1** in peptide **A**. Peptide **M** appears to be incapable of adopting a *β*-sheet structure at pH 8.5, presumably because the Lys residues that flank **1** cannot support the formation of a hydrophobic cluster which appears to be critical for *β*-sheet nucleation (Figure 8).[5a] The aliphatic portion of the Lys side chain does not appear to interact with the dibenzofuran skeleton to form a stable hydrophobic cluster, probably because the aliphatic chain is simply not bulky enough to make sufficient van der Waals contact with the dibenzofuran ring system (see below). Under more alkaline conditions (>pH 8.5), this peptide is capable of folding to afford a *β*-sheet structure whose CD spectrum is very similar to that of peptide **A** at pH 8.5. It could be that at pHs > 8.5 the Lys side chain is sufficiently neutralized to better pack against the dibenzofuran skeleton. Ongoing experiments may provide insight into the folding of peptide **M** at high pH.

A detailed study carried out previously employing a series of related heptapeptides incorporating **1** suggests that a hydrophobic cluster composed of the dibenzofuran skeleton and the hydrophobic side chains of the flanking amino acid residues is required for *β*-sheet nucleation.[5a] Further evidence for the presence and importance of the hydrophobic cluster can be seen from the near-UV CD analysis of peptides **A** and **M**. A comparison of the near-UV CD spectra of these two peptides at pH 8.5 reveals that peptide **M** does not exhibit a dibenzofuran derived near-UV CD signal whereas peptide **A** does (Figure 9),

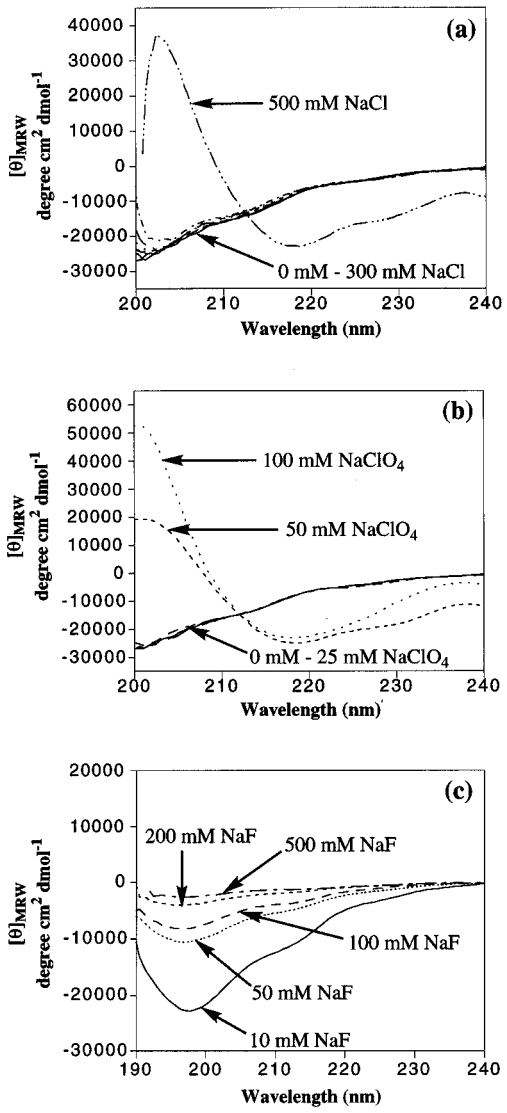

Figure 6. Salt dependent far-UV CD spectra of 0.1 mM peptide **A** at pH 4.0 in varying concentrations of (a) NaCl, (b) $NaClO_4$, and (c) NaF in 10 mM acetate buffer (pH 4.0).

suggesting that the lack of a hydrophobic cluster explains peptide **M**'s inability to fold. The near-UV CD spectrum exhibited by peptide **A** at pH 8.5 dictates that the dibenzofuran chromophore is in a rigid chiral environment. On the basis of equilibrium ultracentrifugation data (vide infra), it is likely that the near-UV CD signal at this pH results from intramolecular hydrophobic cluster contributions as well as contributions from the β-sheet quaternary structure. Importantly, circular dichroism studies also reveal that peptide **A** exhibits a near-UV CD spectrum at low pH (4.0) where a random coil far-UV CD spectrum is observed (Figure 10), implying that the hydrophobic cluster can exist under conditions which do not favor strand interactions. The near-UV CD spectrum obtained at pH 4 is different from that obtained at pH 8.5 in that it is much less intense and has a different wavelength dependence, supporting the idea that there are both intra- and intermolecular contributions to the near-UV CD spectra of peptide **A** at pH 8.5. Equilibrium ultracentrifugation experiments demonstrate that peptides **A** and **M** are both monomeric at pH 4.0. These results suggest that it is the hydrophobic cluster present in peptide **A** that is poised to nucleate folding once the charge density is diminished in the strands that must interact to form the intramolecularly folded β-sheet. The stability of the dibenzofuran mediated hydrophobic cluster is similar to protein-based hydrophobic clusters which remain intact even under conditions where the protein is considered "unfolded", i.e., at low pH or in the presence of chaotropic agents, e.g., urea.[17] In the case of the amino-terminal 63-residue domain of the 434-repressor, a hydrophobic cluster consisting of residues **54**−**59** was found to be stable in a 7 M urea solution as discerned by NOE experiments.[17f] Similarly, peptide **A** exhibits a near-UV CD spectrum at pH 4.0 in 9.15 M urea, Figure 11, consistent with the proposal that the hydrophobic cluster is poised and ready to nucleate sheet folding once solution conditions facilitate strand interactions. It is likely that these hydrophobic clusters act as nucleation sites which guide the initial steps of folding and constrain the chain topology so that the polypeptide can fold properly into its preprogrammed native three dimensional structure.[17]

Comparative NMR studies were performed on peptides **A** and **M** to provide further evidence for the presence of the hydrophobic cluster under conditions where strand collapse in peptide **A** is unfavorable. A simple 1D NMR spectrum was recorded for peptide **A** at pH 4.5 where the peptide lacks β-sheet structure. The NMR spectrum exhibited by peptide **A** shows that the methyl proton signals from the valine residues flanking **1** are shifted upfield by ca. 0.3 ppm relative to the other valine residues in the sequence, Figure 12a. A slightly smaller upfield shift of the methyl protons in the flanking Val residues in peptide **A** is also observed at pH 4.5 in 9 M urea, Figure 12b. The upfield shift observed for the diastereotopic methyl groups of the flanking Val-6 and Val-9 residues appears to result from hydrophobic cluster formation which places the side chain methyl groups in the shielding cone of the dibenzofuran skeleton. The NMR results confirm the conclusions drawn from the near-UV CD results, indicating that the hydrophobic cluster created by **1** and the flanking α-amino acid residues is a relatively stable structure and is necessary for β-sheet folding. As a control, peptide **M** was also analyzed by NMR at pH 4.5 (data not shown). The spectrum of peptide **M** does not appear to exhibit any upfield shifted methylene protons which would result if the aliphatic portion of the Lys side chain was interacting with the face of the dibenzofuran ring. The NMR data embrace the conclusions drawn from the near-UV CD studies on peptide **M**, which indicate that a hydrophobic cluster is not formed in this peptide below pH 8.5. The inability of peptide **M** to form a hydrophobic cluster appears to explain why this peptide does not adopt a β-sheet structure at pH 8.5.

Further characterization of the hydrophobic cluster present in peptide **A** was accomplished by a 2D ROESY NMR experiment at pH 4.5 which identified NOEs characteristic of interactions between the dibenzofuran skeleton and the methyl groups of the flanking Val residues. The ROESY experiment identifies NOEs between the dibenzofuran protons and the Val methyl protons, indicating that the hydrophobic Val side chains are in close proximity to the dibenzofuran ring consistent with the hydrophobic cluster conformation. These data support the existence and importance of the hydrophobic cluster mediated by **1** in the folding of peptide **A**. In other words the hydrophobic cluster is always present and poised to nucleate folding in peptide **A**.

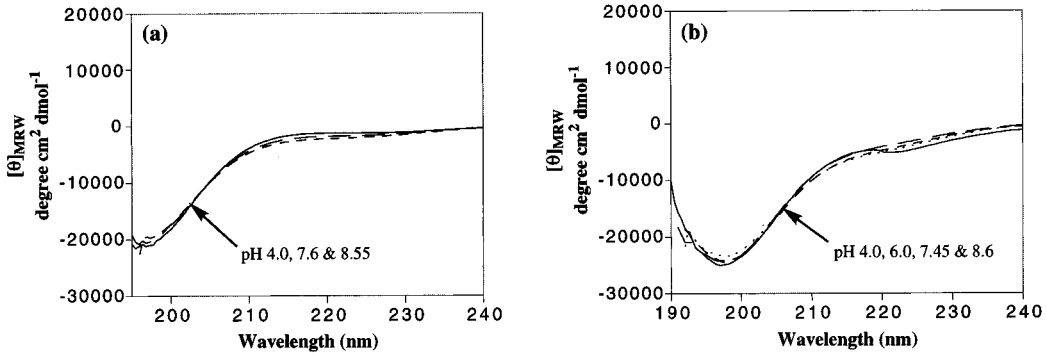

Figure 7. Far-UV CD spectra of (a) 0.35 mM peptide **K** and (b) 0.2 mM peptide **L** as a function of pH using 10 mM acetate buffer (at pH 4.0 and 6.0), 10 mM Tris buffer (at pH 7.5), and 10 mM borate buffer (at pH 8.5).

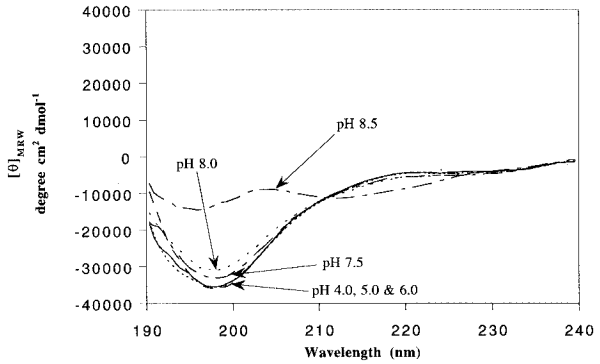

Figure 8. Far-UV CD spectra of 0.1 mM peptide **M** as a function of pH.

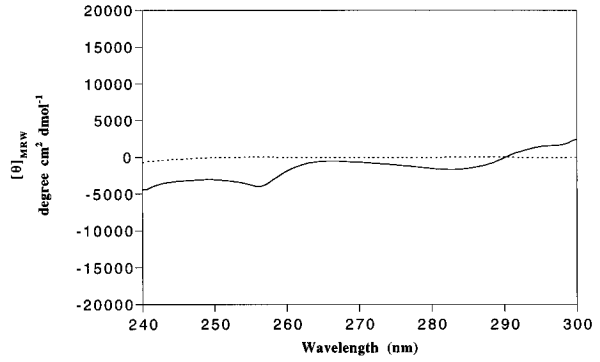

Figure 9. Comparative near-UV CD spectra at pH 8.5 of 0.1 mM peptide **A** (—) and 0.1 mM peptide **M** (- -) in 10 mM borate buffer (pH 8.5).

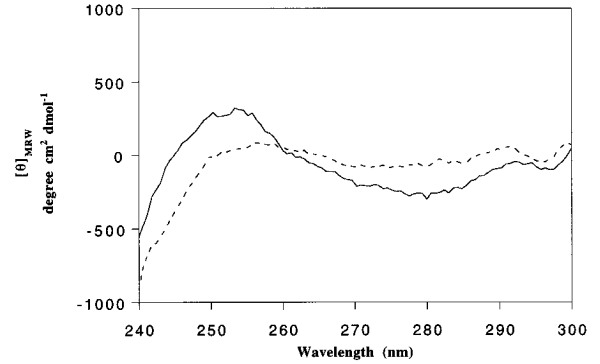

Figure 10. Comparative near-UV CD spectra of 0.1 mM peptide **A** (—) and peptide **M** (- -) in 10 mM acetate buffer (pH 4.0).

A pH dependent UV analysis was performed on peptide **A** to determine if the formation of the hydrophobic cluster could be monitored through changes in the electronic spectra of the dibenzofuran chromophore.

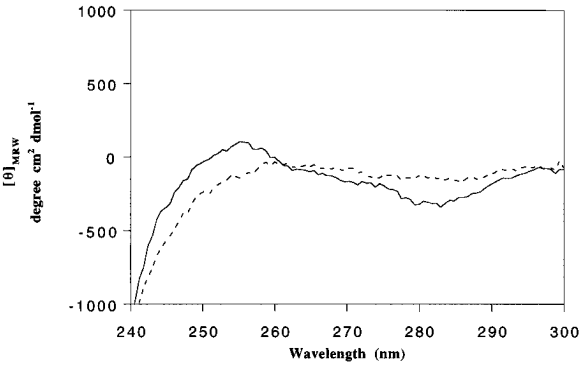

Figure 11. Comparative near-UV CD spectra of 0.1 mM peptide **A** (—) and 0.1 mM peptide **M** (- -) in 10 mM acetate buffer, 9.15 M urea (pH 4.0).

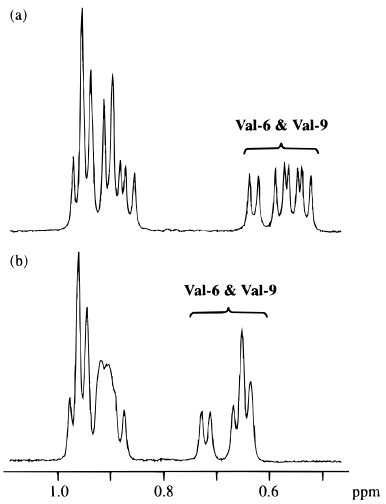

Figure 12. 1D NMR spectra of the Val aliphatic side chain region of (a) peptide **A** in deuterated acetate buffer 90:10% H_2O: D_2O (pH 4.5) at 25 °C and (b) peptide **A** with 9 M urea in deuterated acetate buffer 90:10% H_2O: D_2O (pH 4.5) at 25 °C. Note the significant upfield shift of the Val-6 and Val-9 methyl groups relative to those of the remaining Val residues in peptide **A**. The upfield shift further supports the hydrophobic cluster conformation adopted by the Val-6-**1**-Val-9 tripeptide unit in peptide **A**.

The UV spectrum of this peptide exhibits hyperchromicity and a red shift in the dibenzofuran absorption as the pH is increased from 4.0 to 8.5, Figure 13. All these effects are indicative of a change in the environment around the aromatic ring system. However, it is not likely that these effects are due entirely to the formation of the hydrophobic cluster because it has been determined that the cluster exists even in the "unfolded state" of peptide **A**. On the basis of the equilibrium

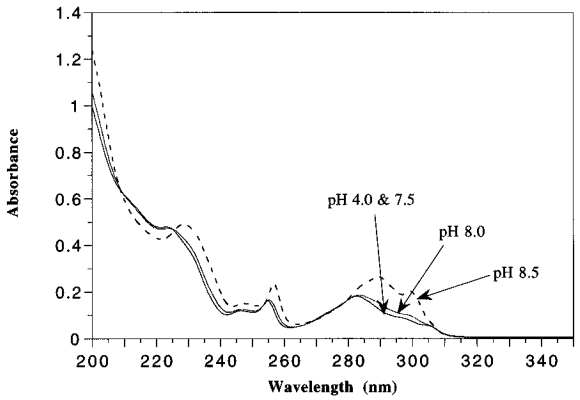

Figure 13. UV spectra of 0.1 mM peptide **A** as a function of pH using 10 mM acetate buffer (pH 4.0) and 10 mM borate buffer (pH 7.5, 8.0, and 8.5). The spectra were corrected for buffer contributions.

ultracentrifugation results which indicate that peptide **A** is associated at pH 8.5 (vide infra), it seems more probable that the UV changes are largely a consequence of the association process and do not report on the presence of the hydrophobic cluster.

Quaternary Structure Determination of Structured Peptide A. It is apparent from the comparisons between peptides **A**−**M** that intramolecular folding mediated by residue -Val-**1**-Val- is important for β-sheet formation in peptide **A**. The question to be addressed here is to what extent does the peptide self-associate after folding occurs. On the basis of the amphiphilicity of the folded β-sheet structure of peptide **A**, it is expected that the individual sheets would subsequently dimerize through association of their hydrophobic faces to generate a dimeric β-sandwich structure which may laterally associate via intermolecular β-sheet formation to form a high MW assembly (vide supra).

Analytical equilibrium ultracentrifugation was employed to reliably establish the quaternary structure adopted by peptide **A** as a function of pH.[18a] Both sedimentation equilibrium and sedimentation velocity experiments prove useful for analyzing quaternary structure in aqueous solution.[18a,b] The concentration of a peptide at equilibrium under the influence of a centrifugal field as a function of radial distance in the centrifuge can be fit to a single exponential of the following type: $c(r) = c_h e^{AN(r^2-r_h^2)}$, where r is a given radial position, c_h is the concentration (g/L) at a given radial reference position (r_h) in the cell, N is the apparent molecular weight of the solute, and A is a constant defined as $A = 1 - \bar{\nu}\rho\varpi^2/(2RT)$, where $\bar{\nu}$ is the partial specific volume, ρ is the solution density, ϖ is the angular velocity (rad/s), R is the gas constant, and T is absolute temperature. Peptide **A** was determined to be monomeric at pH 4.0 from a fit to the experimental data using an reasonable value for $\bar{\nu}$ of 0.82 which affords a MW of 1605 (expected MW = 1645). Peptide **A** does not behave as a simple dimeric system at pH 8.5. Rather, the soluble β-sheet structure observed at pH 8.5 presumably results from further association of the putative dimeric β-sheet sandwich into a high-molecular weight β-sheet quaternary structure as determined by the rapid sedimentation of this peptide to the bottom of the ultracentrifuge cell in a relatively short period of time (2−3 h) at a rotor speed of 26 000 rpm. Peptide **A** was subsequently analyzed by analytical equilibrium ultracentrifugation over a concentration range of 8−25 μM. Even at low concentrations, peptide **A** still has a tendency to form high-molecular weight assemblies, implying that the K_D for self-association is sub-micromolar.

In an effort to obtain a species which could be more readily analyzed by analytical equilibrium ultracentrifugation, an attempt was made to control the degree of association of peptide **A**. It was hoped that intermediate concentrations of urea would reduce some of the intersheet mediated interactions while allowing the intrasheet interactions to remain unperturbed (vide infra). The results of these experiments fall into two categories: either peptide **A** is observed to be highly associated (low urea concentrations) or the peptide is observed to be monomeric and denatured. On the basis of these results, it appears that urea solutions are not useful for affording a well-defined quaternary form of peptide **A**. Since urea was not effective in controlling the association of peptide **A**, we considered studying peptide **A** under conditions where the pH mediated conversion from a random coil to a β-sheet was only partially complete. In this study three pH's were considered, 8.0, 8.1, and 8.25. It was observed that as the pH increased, less peptide was left in solution after ultracentrifugation. In addition, the apparent molecular weight calculated for the peptide remaining in solution specifies a monomer species at each pH. These results are consistent with the idea that an equilibrium exists between folded and unfolded states of peptide **A** and that the folded state of peptide **A** self-associates into a large β-sheet quaternary structure that sediments from the ultracentrifugation cell at micromolar concentrations. The metastable folded state of peptide **A** is likely to be a face to face dimeric β-sandwich, but this cannot be demonstrated at the current time. Self-association of the dimer most likely occurs through extensive lateral hydrogen bonding between intramolecularly folded β-sheet sandwiches. In summary, the folding and self-association equilibria are linked.

The ultracentrifugation studies suggest that urea denatures the β-sheet assembly formed by peptide **A**. In order to utilize urea denaturation as a means of measuring the stability of the self-assembled form of peptide **A** in solution, it is necessary to determine that the unfolding of this peptide by urea is reversible. It was demonstrated by far-UV CD that peptide **A** (0.1 mM at pH 8.5) adopts a random coil conformation in 7 M urea. Upon dilution of this 7 M solution to 1 M urea, peptide **A** exhibited a β-sheet signal which was identical to that of a control peptide solution (0.1 mM peptide **A** at pH 8.5) incubated exclusively in 1 M urea, establishing reversiblility. The urea induced denaturation of peptide **A** was monitored by measuring the ellipticity at 220 nm as a function of urea concentration, Figure 14a.[25] Determination of the K_{eq} between the associated β-sheet structure and the unfolded state as a function of urea concentration affords ΔG as a function of urea concentration. Linear extrapolation of the ΔG as a function of urea concentration back to zero denaturant concentration affords ΔG_{H_2O}(apparent), Figure 14b.[25] The ΔG_{H_2O}(apparent) for peptide **A** is equal to 3.25 kcal/mol, which is less than the 5−15 kcal/mol exhibited by most proteins;[1] however, it is critical to keep in mind that this is the apparent stability of a soluble associated β-sheet. This result demonstrates that the linked folding and self-association steps are reversible.

Structural Evaluation of Precipitates of Peptide A. The above studies have been performed over a pH range of 4.0−8.5 where peptide **A** and analogues thereof are soluble. A light scattering analysis was employed

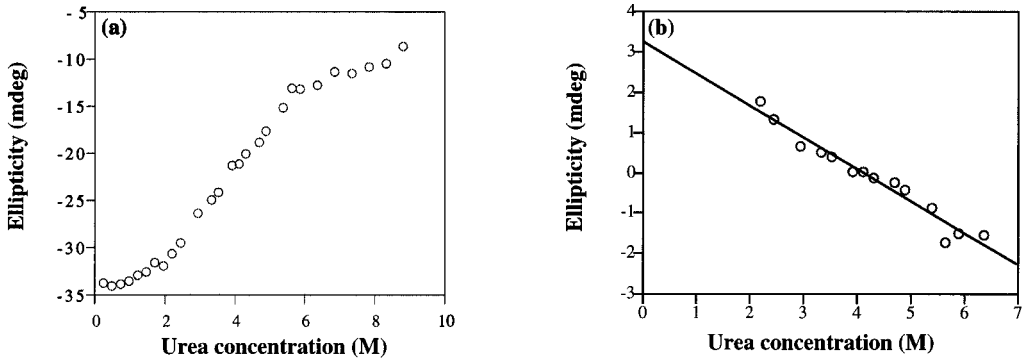

Figure 14. (a) Urea denaturation curves for a 0.1 mM solution of peptide **A** at pH 8.5 in 150 mM NaCl. (b) ΔG_{H_2O}(apparent) plot for peptide **A**.[25]

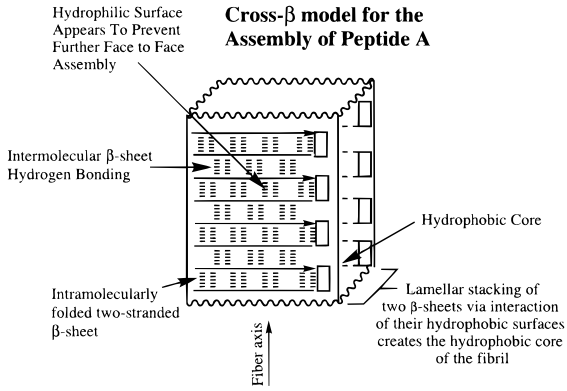

Figure 15. Schematic representation of the cross-β conformation. This assembly presumably forms by the self-association of a dimeric face-to-face β-sheet sandwich via intermolecular β-sheet formation.

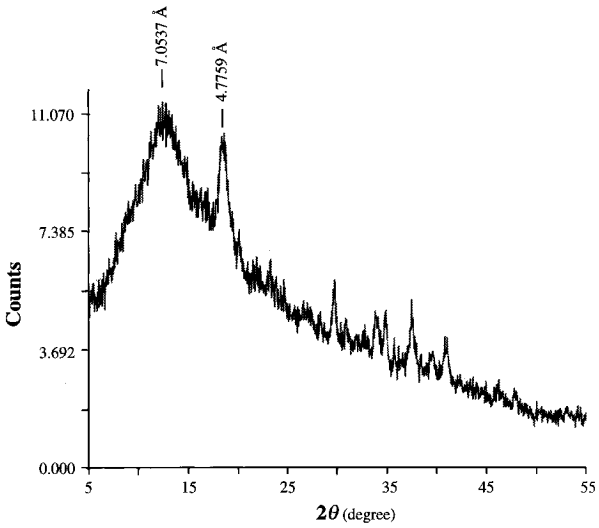

Figure 16. X-ray powder diffraction pattern of peptide **A** precipitated from alkaline solution at pH 11.

to identify the pH at which precipitation would occur and to determine whether this aggregation/precipitation process is reversible. Peptide **A** is completely insoluble at pHs $\geq$ 11.0 as discerned from analysis of the supernatant after centrifugation of the precipitate (minifuge). At pH 11 it is likely that most or all of the charges on the Lys side chains have been neutralized, since this pH exceeds the pK_a expected for the ϵ-ammonium groups. Interestingly, when the pH 11 suspension of peptide **A** was treated with 6 M HCl to lower the pH to approximately 3.0, peptide **A** was completely resolublized as discerned by UV spectroscopy . The reversibility of this assembly process indicates that the titratible ϵ-ammonium groups remain solvent exposed and can be easily titrated even in the precipitated state. The reversibility of the β-sheet quaternary structure formation is in agreement with the proposal that peptide **A** first folds intramolecularly, affording a β-sheet structure which subsequently dimerizes as a result of hydrophobic surface interactions affording a β-sheet sandwich having the **Lys** side chain bearing surfaces solvent exposed.[8] The putative metastable dimeric β-sheet apparently self-assembles via intermolecular β-sheet formation to form what may be a cross-β fibril structure, Figure 15.[11,19]

X-ray Powder Diffraction and Electron Microscopy Analyses. X-ray powder diffraction and electron microscopy experiments were employed to further understand the structure of peptide **A** and to provide evidence for or against a β-sheet-sandwich structural motif. X-ray powder diffraction serves to identify the distinctive spacings characteristic of the repeating motifs in a structure. The putative cross-β-conformation of amyloid exhibits an X-ray diffraction pattern having two prevalent spacings at 4.7 Å and ca. 9−10 Å, which correspond to the distance between two interacting β-strands and the perpendicular distance between two face to face associated β-pleated sheets, respectively.[11,20] The precipitate of peptide **A**, generated under alkaline conditions (pH 11), shows a prominent reflection at 4.77 Å, indicative of the strand to strand distance within a β-sheet structure (Figure 16). The other major reflection observed at 7.05 Å is consistent with the distance between the β-sheet planes which are separated by the interacting Val side chains. These data imply that the hydrophilic surfaces of the β-pleated sheets do not pack against one another, since we only observe one sheet to sheet distance expected for interaction of the hydrophobic surfaces of identical β-sheets. These data and the fact that the pH mediated precipitation of peptide **A** is reversible argue in favor of a structure similar to that presented in Figure 15, where the fibrils are two β-sheets thick as a result of exposed hydrophilic Lys residues.

Electron microscopy has been widely used to determine the overall structural morphology of amyloid protein deposits which appear to have a cross-β-fibril structure.[11,20] Because peptide **A** and analogues thereof form both soluble and insoluble high-molecular weight β-sheet structure(s), electron microscopy was employed to compare its structural morphology to that exhibited by amyloid. Peptide **G**, a trifluoroacetylated analogue of peptide **A**, was selected for this experiment because it can form a soluble β-sheet structure in solution at pH 4.0 (150 mM NaCl). The putative soluble fibril was

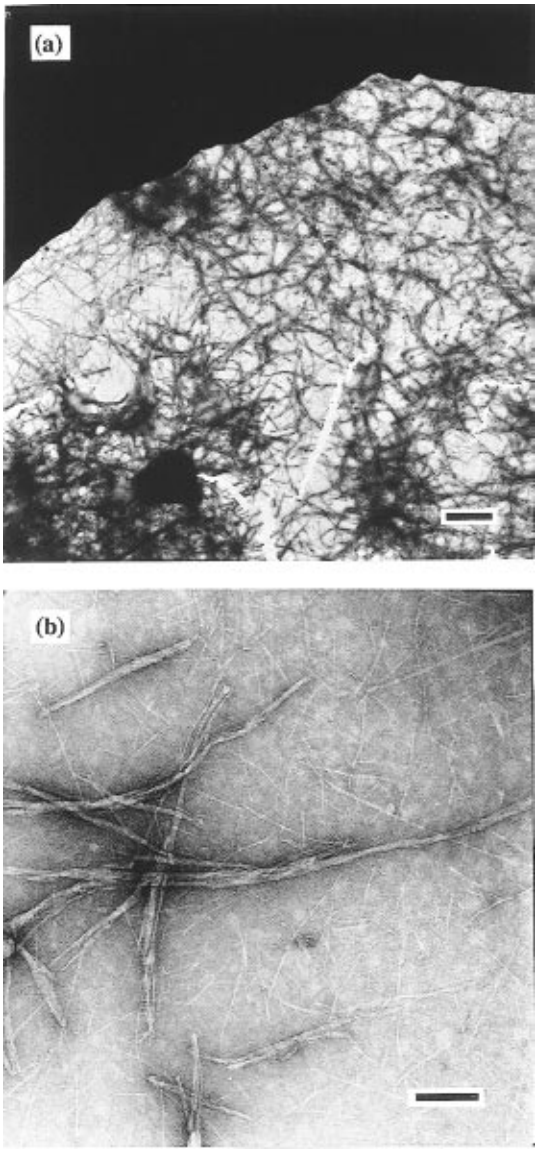

Figure 17. (a) Electron micrograph of negatively stained (1% uranyl acetate) fibrils from a solution of 0.1 mM peptide **G** at pH 4.0; magnification 10000× (reproduced at 65% of original size); bar, 5000 Å. (b) Electron micrograph of negatively stained (1% uranyl acetate) fibrils from a solution of 0.0125 mM peptide **G** at pH 4.0; magnification 63000× (reproduced at 65% of original size); bar, 1000 Å.

absorbed onto a carbon coated copper grid and stained with uranyl acetate at pH 4. Fibrillar structures were observed when the negatively contrasted samples of peptide **G** were examined, Figure 17a. Measurements carried out on the smallest fibril structure exhibited by peptide **G** yields a structure of ≈30 Å in width by several hundred nanometers in length. A CPK model of peptide **G** in a cross-β-sheet conformation analogous to that shown in Figure 15 indicates that the width in the β-strand direction is ≈28 Å, comparable to the width of the fibrils of peptide **G** as discerned by electron microscopy. This measurement is consistent with fibrils having a cross-β conformation; however, the orientation of the peptide strand relative to the fibril axis is still under scrutiny. The electron micrographs also clearly indicate the presence of higher ordered fibril assemblies which are also under further study. The electron microscopy data on peptide **G** suggest that peptide **A** and its analogues also form a soluble β-fibril structure in aqueous solution.

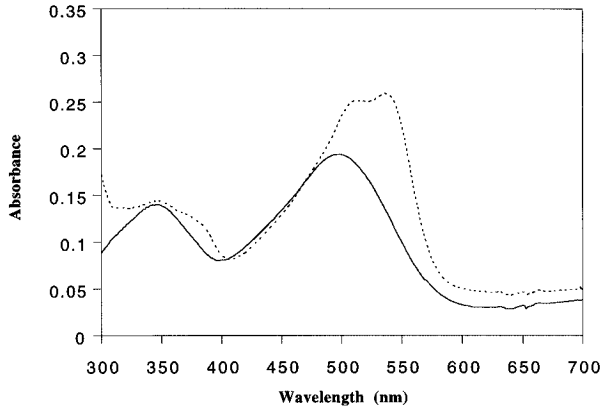

Figure 18. UV spectra of 4.75 μM Congo red at pH 11 in the absence (—) and presence of (- -) 5 μM peptide **A**. The spectra were corrected for buffer contributions.

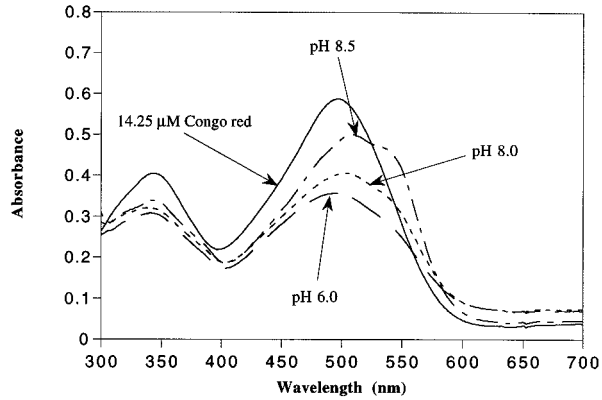

Figure 19. pH dependent UV profile of 14.25 μM Congo red in the presence of 5 μM peptide **A** using 10 mM acetate buffer (pH 6.0), 10 mM Tris buffer (pH 7.5 and 8.0), and 10 mM borate (pH 8.25 and 8.5). The spectra were corrected for buffer contributions.

Congo Red Binding and Birefringence Analyses. In order to compare the quaternary structure of peptide **A** to the cross-β-structures formed from insulin and amyloid proteins, Congo red binding and birefringence studies were carried out on peptide **A**. Congo red is a sulfonated azo dye which binds preferentially, but not exclusively, to protein and polypeptide species adopting a cross-β-structure (e.g., amyloid).[21] Figure 18 demonstrates that, at pH 11, a suspension containing precipitates of peptide **A** is able to bind Congo red as evident by the characteristic hyperchromicity and a red shift in the UV spectrum of bound Congo red. A closer examination reveals that the UV spectrum of Congo red bound to peptide **A** is very similar to the spectrum exhibited by Congo red bound to poly-L-lysine (β-pleated sheet form). Both spectra exhibit double maxima at approximately 512 and 536 nm.[21c] The insoluble fibrils of peptide **A** containing bound Congo red were subsequently subjected to analysis under a polarizing microscope and were found to exhibit green birefringence upon rotation of the plane of the polarized light by 90°. This phenomenon, which is also seen in Congo red stained amyloid fibrils, provides additional evidence for the presence of a regular quaternary structure consistent with a cross-β-sheet quaternary structure.[22] Interestingly, even under conditions where peptide **A** is soluble (pH 8.0−8.5), Congo red binds strongly to peptide **A**, supporting the existence of a soluble amyloid-like β-fibril structure in solution, Figure 19. The pH dependent Congo red binding behavior exhibited by peptide **A** from pH 8.0−8.5 is consistent with the linked

folding and self-association equilibria which govern the appearence of β-sheet structure.

Summary

The aromatic amino acid residue **1** nucleates intramolecular antiparallel β-sheet folding in tridecapeptides which subsequently self-assemble into β-sheet fibrils, perhaps having a cross-β-conformation. Residue **1** functions as a folding nucleator by facilitating intramolecular hydrogen bonding between the flanking α-amino acid residues and by favoring the formation of a hydrophobic cluster composed of the dibenzofuran skeleton and hydrophobic side chains of the flanking α-amino acids. The template facilitates intramolecular folding in peptides such as peptide **A**, which subsequently undergo lateral self-assembly such that the folding and self-association equilibria are linked. Together, the X-ray diffraction data, the electron microscopy results, and the Congo red binding studies support the existence of a β-sandwich-type fibrillar structure in peptide **A** and its analogues. The template strategy described for producing fibrils allows significant α-amino acid sequence variations to be accommodated in the resulting β-sheet-based macromolecular assembly without interfering with the folding/assembly pathway, since it is the template interacting with the flanking α-amino acids which serves to nucleate folding. From this preliminary study it appears that template directed folding should be useful for the preparation of self-assembling architectures or nanostructures.

Experimental Section

Details regarding peptide synthesis and purification can be found in the supplemental material and in refs 5a, 23, and 28.

Summary of Purification and Characterization of Peptides A−M. Peptide A ($C_{83}H_{144}N_{20}O_{14}$). Purified using a 20 min gradient from 20 to 50% **B**; 230 mg (27% yield). MALDI-TOFMS m/z (MH^+): calcd, 1646.1; obsd, 1646.6.

Peptide B ($C_{85}H_{146}N_{20}O_{15}$). Purified using a 20 min gradient from 20 to 50% **B**; 550 mg (39% yield). MALDI-TOFMS m/z (MH^+): calcd, 1688.1; obsd, 1688.1.

Peptide C ($C_{85}H_{143}N_{20}O_{15}F_3$). Purified using a 20 min gradient from 25 to 45% **B**; 120 mg (14% yield). MALDI-TOFMS m/z (MH^+): calcd, 1742.1; obsd, 1742.4.

Peptide D ($C_{85}H_{143}N_{20}O_{15}F_3$). Purified using a 20 min gradient from 25 to 45% **B**; 113 mg (13% yield). MALDI-TOFMS m/z (MH^+): calcd, 1742.1; obsd, 1742.1.

Peptide E ($C_{85}H_{143}N_{20}O_{15}F_3$). Purified using a 20 min gradient from 25 to 45% **B**; 130 mg (15% yield). MALDI-TOFMS m/z (MH^+): calcd, 1742.1; obsd, 1742.6.

Peptide F ($C_{85}H_{143}N_{20}O_{15}F_3$). Purified using a 20 min gradient from 25 to 45% **B**; 228 mg (27% yield). MALDI-TOFMS m/z (MH^+): calcd, 1742.1; obsd, 1741.9.

Peptide G ($C_{87}H_{142}N_{20}O_{16}F_6$). Purified using a 20 min gradient from 30 to 55% **B**; 129 mg (15% yield). MALDI-TOFMS m/z (MH^+): calcd, 1838.1; obsd, 1837.9.

Peptide H ($C_{87}H_{142}N_{20}O_{16}F_6$). Purified using a 25 min gradient from 20 to 50% **B**; 260 mg (31% yield). MALDI-TOFMS m/z (MH^+): calcd, 1838.1; obsd, 1838.5.

Peptide I ($C_{87}H_{142}N_{20}O_{16}F_6$). Purified using a 25 min gradient from 20 to 50% **B**; 181 mg (21% yield). MALDI-TOFMS m/z (MH^+): calcd, 1838.1; obsd, 1838.0.

Peptide J ($C_{87}H_{142}N_{20}O_{16}F_6$). Purified using a 25 min gradient from 20 to 50% **B**; 140 mg (17% yield). MALDI-TOFMS m/z (MH^+): calcd, 1838.1; obsd, 1838.1.

Peptide K ($C_{70}H_{135}N_{21}O_{14}$). Purified using a 20 min gradient from 0 to 45% **B**; 180 mg (27% yield). MALDI-TOFMS m/z (MH^+): calcd, 1495.1; obsd, 1495.1.

Peptide L ($C_{80}H_{145}N_{21}O_{14}$). Purified using a 20 min gradient from 0 to 30% **B**; 83 mg (16% yield). FABMS m/z (MH^+): calcd, 1625.7; obsd, 1626.0.

Peptide M ($C_{83}H_{144}N_{20}O_{14}$). Purified using a 20 min gradient from 20 to 50% **B**; 160 mg (22% yield). MALDI-TOFMS m/z (MH^+): calcd, 1646.1; obsd, 1647.1.

UV Analysis. All UV analyses were carried out on a Milton Roy Spectronic 3000 diode array spectrophotometer. UV spectra were recorded prior to CD studies in order to determine the concentration of peptide stock solutions using the dibenzofuran chromophore (ϵ_{282nm} = 17 797 cm^{-1} M^{-1}).

Circular Dichroism Studies. All circular dichroism experiments were performed on a Jasco J-600 spectropolarimeter at 25 °C. A weighed amount of peptide was diluted with doubly distilled water to afford a peptide stock solution at pH 4−6. Peptide samples were then prepared by diluting the peptide stock solution with the appropriate buffer to afford the desired peptide concentration as determined by UV analysis. The pH of each sample solution was remeasured and adjusted if necessary. The samples were subsequently degassed by sonication under a water aspirator vacuum and then incubated for 24 h at 25 °C in a water bath. After incubation, the samples were centrifuged to remove any particulates and the buffer pH rechecked prior to recording the CD spectra. CD data were acquired at a band width of 1.0 nm, a time constant of 0.5 s, and a scan speed of 20 nm/min. The resulting CD spectrum is an average of six scans. The data from the Jasco spectrometer were imported into the Macintosh version of KaleidaGraph, processed, and reported in units of mean residue ellipticity.[24]

pH Dependent CD Studies. All peptide samples were prepared as 0.1−0.35 mM solutions at a specified pH by dilution of a peptide stock solution with 10 mM acetate (for pHs 4−6), 10 mM Tris (where specified), or 10 mM borate buffer (for pHs 7.5−8.5). Corresponding samples were also made in which NaCl was added to afford a salt concentration of 75 mM. The far-UV CD spectrum for each sample was recorded in a 1.0 mm quartz cell from 240 to 190 nm or from 240 to 195 nm when high absorbances prevented collection of data to 190 nm. The spectra were corrected for buffer contributions and are reported in units of mean residue ellipticity.[24]

Urea Denaturation Studies. Each sample was prepared by dilution of the peptide stock solution into a buffered solution at the appropriate urea concentration. All samples were 0.1 mM in peptide, 0.15 M in NaCl, and 50 mM in borate buffer at pH 8.5. Each buffered urea solution was prepared from a urea stock solution whose concentration was determined by weight fraction analysis and refractive index measurements.[25] Buffered urea solutions contained 0.15 M NaCl and 50 mM borate buffer at pH 8.5. The ellipticity value at 220 nm was recorded for each peptide sample as a function of urea concentration in a 1.0 mm quartz cell. The dependence of the ellipticity value on urea concentration was plotted and ΔG_{H_2O} determined as described previously by Pace and Shirley.[25]

Near-UV CD Studies. All samples at pH 4.0 were prepared as 0.3 mM peptide solutions by dilution of a peptide stock solution with 10 mM acetate buffer (pH 4.0). Samples at pH 8.5 were prepared as 0.1 mM peptide solutions by dilution of a peptide stock with 10 mM borate buffer (pH 8.5). The CD spectrum for each sample was recorded in a 1.0 or 5.0 mm quartz cell from 300 to 240 nm.

NMR Studies. The 1D NMR spectra were recorded on a Varian XL 400 spectrometer at 25 °C. All samples were prepared as 5 mM solutions in deuterated 10 mM acetate buffer (pH 4.5). The samples were degassed prior to NMR analysis by sonication under a water aspirator vacuum. The 2D NMR spectra were recorded on a Unity Plus 500 MHz spectrometer. ROESY and NOESY data were recorded as a function of mixing times. A mixing time of 150 ms proved optimal.

Equilibrium Ultracentrifugation Studies. Molecular weight determinations were made on a Beckman XL-A analytical equilibrium ultracentrifuge equipped with absorption optics. A double sector cell equipped with a 12 mm Epon centerpiece and sapphire windows was used for the experiments described within. Samples were loaded into the cell using a blunt end microsyringe, resulting in a column height of approximately 3 mm. Samples were prepared from a

peptide stock solution in water by dilution of an aliquot to the specified concentration utilizing the appropriate buffer solution. The samples were then dialyzed against the same buffer system for 12−24 h at room temperature. The concentration of each dialyzed sample is remeasured by UV spectroscopy and subsequently diluted to its final concentration with the dialysate. In a typical experiment, an initial absorbance scan is performed at a rotor speed of 3000 rpm. The rotor speed is then increased to 42 000 rpm, where sedimentation equilibrium is established. All experiments are run at 23.0 °C. A complete loss of the initial absorbance is indicative of a highly associated system.

Congo Red Binding Studies. A Congo red stock solution was prepared by dissolving the dye in distilled water and filtering the solution three times through a Magna nylon membrane (0.45 μm).[21c] The concentration of the Congo red stock was determined by measuring the absorbance of a diluted aliquot at 477 nm ($\epsilon_{477nm} = 34\ 722\ cm^{-1}\ M^{-1}$). Buffered Congo red solutions at specified concentrations were prepared by dilution of an aliquot of the stock solution with the appropriate buffer solution. Peptide samples for binding studies were prepared from a peptide stock diluted with the appropriate buffer. The peptide samples were then incubated for 24 h at 25 °C. Binding studies were carried out by diluting 100 μL of a peptide solution to 2.0 mL with the appropriate Congo red solution. The resulting solution was then mixed and allowed to incubate at room temperature for 0.5 h. An ultraviolet spectrum was then recorded for the sample mixture from 300 to 700 nm in which a blank containing the appropriate buffer solution with no Congo red was subtracted. Corresponding solutions consisting of buffered Congo red solution were also recorded to serve as control solutions.

Electron Microscopy Studies. A peptide sample was prepared at pH 4 from a stock solution in H_2O at pH 5−6 by dilution with the appropriate buffer. The peptide sample was incubated for 24 h at 25 °C. The sample was then applied to a carbon-coated copper grid for 1−2 min. Excess solution was removed by filter paper blotting. The sample on the grid was then stained with a fresh solution of 1% (w/v) uranyl acetate (pH 4.0) for 1−2 min and the excess staining solution removed. The sample was subsequently visualized with a Zeiss 10C electron microscope operating at 60 kV. With utilization of a slide guide ultrastructure calculator which takes into account the magnification factor at which the electron microscope was set when the electron micrograph was photographed, the fibril dimensions (width and length) are first measured in millimeters and then converted to angstroms. Any enlargement that occurred upon photographic developing of the negative was also taken into account.

X-ray Diffraction Studies. A concentrated solution of peptide **A** in water was adjusted to pH 11 with a concentrated NaOH solution and then allowed to incubate for 24 h at 25 °C. The solution was subsequently lyophilized to afford a white powder. X-ray diffraction patterns were recorded on a Scintag PAD V computer controlled diffractometer. The X-ray source which utilized Cu Kα radiation was operating at 45 kV and 30 mA.

Acknowledgment. We thank Professors Don Albright, Marty Scholtz, and Nick Pace for helpful discussions, Timothy Hayes for allowing us to perform HF cleavages in his laboratory, David Russell for providing access to and assistance with MALDI-TOFMS, and Steve Silber and Robert Espina their help with the NMR experiments. We gratefully acknowledge financial support of the Robert A. Welch Foundation, Searle Scholars Program/The Chicago Community Trust (J.W.K.), the National Institutes of Health (Grant R01 GM51105), the Camille and Henry Dreyfus Foundation Teacher Scholars Program (J.W.K.), and the Center for Macromolecular Design.

Supporting Information Available: Peptide synthesis and purification details as well as far-UV CD spectra of peptides **H**−**J** as a function of pH (5 pages). This material is contained in many libraries on microfiche, immediately follows this article in the microfilm version of the journal, and can be ordered from the ACS; see any current masthead page for ordering information.

References and Notes

(1) (a) Mattice, W. L. *Annu. Rev. Biophys. Biophys. Chem.* **1989**, *18*, 93. (b) Yapa, K.; Weaver, D. L.; Karplus, M. *Proteins: Struct., Funct., Genet.* **1992**, *12*, 237. (c) Dyson, H. J.; Wright, P. E. *Annu. Rev. Biophys. Biophys. Chem.* **1991**, *20*, 519. (d). Liu, Z.-P.; Rizo, J.; Gierasch, L. M. *Biochemistry* **1994**, *33*, 134.

(2) (a) DeGrado, W. F.; Wasserman, Z. R.; Lear, J. D. *Science* **1989**, *243*, 622. (b) Kemp, D. S.; Boyd, J. G.; Muendel, C. C. *Nature* **1991**, *352*, 451. (c) Goodman, E. M.; Kim, P. S. *Biochemistry* **1989**, *28*, 4343. (d) Lyu, P. C.; Marky, L. A.; Kallenbach, N. R. *J. Am. Chem. Soc.* **1989**, *111*, 2733. (e) Poland, D.; Scheraga, H. A. *Theory of Helix-Coil Transitions in Biopolymers*; Academic Press: New York, 1970. (f) Zimm, B. H.; Bragg, J. *J. Chem. Phys.* **1959**, *31*, 526.

(3) (a) Kemp, D. S.; Curran, T. P.; Davis, W. M.; Boyd, J. G.; Muendel, C. C. *J. Org. Chem.* **1991**, *56*, 6672. (b) DeGrado, W. F.; Lear, J. D. *J. Am.. Chem. Soc.* **1985**, *107*, 7684. (c) Zhang, S.; Holmes, T.; Lockshin, C.; Rich, A. *Proc. Natl. Acad. Sci. U.S.A.* **1993**, *90*, 3334. (d) Zhang, S.; Lockshin, C.; Cook, R.; Rich, A. *Biopolymers* **1994**, *34*, 663. (e) Minor, D. L.; Kim, P. S. *Nature* **1994**, *367*, 660. (f) Smith, C. K.; Withka, J. M.; Regan, L. *Biochemistry* **1994**, *33*, 5510. (g) Kim, C.; Berg, J. *Nature* **1993**, *362*, 267.

(4) (a) Hartman, R.; Schwaner, R. C.; Hermans, J, Jr. *J. Mol. Biol.* **1974**, *90*, 415. (b) Brack, A.; Orgel, L. E. *Nature* **1975**, *256*, 383. (c) Brack, A.; Caille, A. *Int. J. Pept. Protein Res.* **1978**, *11*, 128. (d) Brack, A.; Spach, G. *J. Am. Chem. Soc.* **1981**, *103*, 6319. (e) Johnson, B. S. *J. Pharm. Sci.* **1974**, *63*, 313. (f) Maeda, H.; Ooi, K. *Biopolymers* **1981**, *20*, 1549. (g) Maeda, H.; Gatto, Y.; Ikeda, S. *Macromolecules* **1984**, *17*, 2031. (h) Maeda, H. *Bull. Chem. Soc. Jpn.* **1987**, *60*, 3438. (i) Mattice, W. L.; Lee, E.; Scheraga, H. A. *Can. J. Chem.* **1985**, *63*, 140. (j) Rippon, W. B.; Chen, H. H.; Walton, A. G. *J. Mol. Biol.* **1973**, *75*, 369. (k) Seipke, G.; Arfmann, H. A.; Wagner, K. G. *Biopolymers* **1974**, *13*, 1621. (l) Barbier, B.; Caille, A.; Brack, A. *Biopolymers* **1984**, *23*, 2299.

(5) (a) Tsang, K. Y.; Diaz, H.; Graciani, N.; Kelly, J. W. *J. Am. Chem. Soc.* **1994**, *116*, 3988. (b) Graciani, N. R.; Tsang, K. Y.; McCutchen, S. L.; Kelly, J. W. *Bioorg. Med. Chem.* **1994**, *2*, 999. (c) Diaz, H.; Tsang, K. Y.; Choo, D.; Kelly, J. W. *Tetrahedron* **1993**, *49*, 3533. (d) Diaz, H.; Tsang, K. Y.; Choo, D.; Espina, J. R.; Kelly, J. W. *J. Am. Chem. Soc.* **1993**, *115*, 3790. (e) Diaz, H.; Espina, J. R.; Kelly, J. W. *J. Am. Chem. Soc.* **1992**, *114*, 8316.

(6) The incorporation of one strategically placed N-methylated amino acid residue into each strand of peptide **A** affords a monomeric β-sheet structure as discerned from 2D-NMR and far-UV CD studies.

(7) For a review on the utility of templates as folding initiators for monomeric protein-like structures, see: Schneider, J. P.; Kelly, J. W. *Chem. Rev.* **1995**, *95*, 2169.

(8) (a) Tanford, C. *The Hydrophobic Effect;* Wiley: New York, 1973; p 200. (b) Kaiser, E. T.; Kezdy, F. J. *Science* **1984**, *223*, 249.

(9) Kaplan, D., Adams, W. W., Farmer, B., Viney, C., Eds. *Silk Polymers*; ACS Symposium Series 544; American Chemical Society: Washington, D.C., 1994.

(10) (a) Krejchi, M. T.; Atkins, E. D. T.; Waddon, A. J.; Fournier, M. J.; Mason, T. L.; Tirrell, D. A. *Science* **1994**, *265*, 1427. (b) Beavis, R. C.; Chait, B. T.; Creel, H. S.; Fournier, M. J.; Mason, T. L.; Tirrell, D. A. *J. Am. Chem. Soc.* **1992**, *114*, 7584. (c) McGrath, K. P.; Fournier, M. J.; Mason, T. L.; Tirrell, D. A. *J. Am. Chem. Soc.* **1992**, *114*, 727. (d) Dougherty, M. J.; Kothakota, S.; Mason, T. L.; Tirrell, D. A. Fournier, M. J. *Macromolecules* **1993**, *26*, 1779. (e) Lotz, B.; Keith, H. D. *J. Mol. Biol.* **1971**, *61*, 195. (f) Lotz, B. *J. Mol. Biol.* **1971**, *61*, 201. (g) Anderson, J. P.; Capello, J.; Martin, D. C. *Biopolymers* **1994**, *34*, 1049. (h) Fraser, R. D. B.; MacRae, T. P.; Stewart, F. H. C.; Suzuli, E. *J. Mol. Biol.* **1965**, *11*, 706. (i) Manuscripts in ref 9.

(11) (a) Glenner, G. G.; Ein, D.; Eanes, E. D.; Bladen, H. A.; Terry, W.; Page, D. L. *Science* **1971**, *174*, 712. (b) Kirschner, D. A.; Abraham, C.; Selkoe, D. J. *Proc. Natl. Acad. Sci. U.S.A.* **1986**, *83*, 503. (c) Halverson, K.; Fraser, P. E.; Kirschner, D. A.; Lansbury, P. T. *Biochemistry* **1990**, *29*, 2639.

(12) Replacement of the Lys-3 and Lys-12 residues in peptide **A** by Thr also affords a pH independent β-sheet structure under identical conditions.
(13) Data are shown in the supplementary material.
(14) (a) Goto, Y.; Takahashi, N.; Fink, A. *Biochemistry* **1990**, *29*, 3480. (b) Goto, Y.; Calciano, L. J.; Fink, A. *Proc. Natl. Acad. Sci. U.S.A.* **1990**, *87*, 573. (c) Goto, Y.; Nishikiori, S. *J. Mol. Biol.* **1991**, *218*, 387. (d) Goto, Y.; Hagihara, Y. *Biochemistry* **1992**, *31*, 732. (e) Goto, Y.; Aimoto, S. *J. Mol. Biol.* **1991**, *218*, 387.
(15) Djerde, D. T.; Schmuchler, G.; Fritz, J. S. *J. Chromatogr.* **1980**, *187*, 35. (b) Gregor, H. P.; Belle, J.; Marcus, R. A. *J. Am. Chem. Soc.* **1955**, *77*, 2713.
(16) Collins, K. D.; Washabaugh, M. W. *Q. Rev. Biophys.* **1985**, *18*, 323.
(17) (a) Dill, K. A.; Chan, H. S. *Proc. Natl. Aca. Sci. U.S.A.* **1990**, *87*, 6388. (b) Evans, P. A.; Topping, K. D.; Wollfson, D. N.; Dobson, C. M. *Proteins: Struct., Funct., Genet.* **1991**, *9*, 248. (c) Garvey, E. P.; Swank, J.; Matthews, C. R. *Proteins: Struct., Funct., Genet.* **1989**, *6*, 259. (d) Lumb, K. J.; Kim, P. S. *J. Mol. Biol.* **1994**, *236*, 412. (e) Rose, G. D.; Roy, S. *Proc. Natl. Acad. Sci. U.S.A.* **1980**, *77*, 4643. (f) Neri, D.; Billeter, M.; Wider, G.; Wüthrich, K. *Science* **1992**, *257*, 1559. (g) Topping, K. D.; Evans, P. A.; Dobson, C. M. *Proteins* **1991**, *9*, 246.
(18) (a) Ralston, G. *Introduction to Analytical Ultracentrifugation*; Beckman Instruments: Fullerton, CA, 1993; p 86. (b) Adams, E. T., Jr.; Tang, L. H.; Sarquis, J. L.; Barlow, G. H.; Norman, W. M. In *Physical Aspects of Protein Interactions*; Catsimpoolas, Ed.; Elsevier−North Holland: New York, 1978; pp 1−55.
(19) (a) Marsh, R. E.; Corey, R. B.; Pauling, L. *Acta Crystallogr.* **1955**, *8*, 710. (b) Geddes, A. J.; Parker, K. D.; Atkins, E. D. Y.; Beighton, E. *J. Mol. Biol.* **1968**, *32*, 343.
(20) Caputo, C. B.; Fraser, P. E.; Sobel, I.; Kirschner, D. A. *Arch. Biochem. Biophys.* **1992**, *292*, 199.
(21) (a) Cooper, J. H. *Lab. Invest.* **1974**, *31*, 232. (b) Glenner, G. G.; Eanes, E. D.; Page, D. L. *J. Histochem. Cytochem.* **1972**, *20*, 821. (c) Klunk, W. E.; Pettegrew, J. W.; Abraham, D. J. *J. Histochem. Cytochem.* **1989**, *37*, 1273. (d) Klunk, W. E.; Pettegrew, J. W. *J. Histochem. Cytochem.* **1989**, *37*, 1293. (e) Puchtler, H.; Sweat, F.; Levine, M. *J. Histochem. Cytochem.* **1962**, *10*, 355. (f) Turnell, W. G.; Finch, J. T. *J. Mol. Biol.* **1992**, *227*, 1205.
(22) Wolman, M.; Bubis, J. J. *Histochemie* **1965**, *4*, 351.
(23) Chait, B. T.; Kent, S. B. H. *Science* **1992**, *257*, 1885, and references cited therein.
(24) Schmid, F. X. In *Protein Structure: a Practical Approach*; Creighton, T. E., Ed.; IRL Press: New York, 1989; p 251.
(25) Pace, C. N.; Shirley, B. A. In *Protein Structure: a Practical Approach*; Creighton, T. E., Ed.; IRL Press: New York, 1989; p 311.
(26) Robinson, D. G.; Ehlers, U.; Herken, R.; Herrmann, B.; Mayer, F.; Schurmann, F.-W. *Methods of Preparation for Electron Microscopy: An Introduction for the Biomedical Sciences*; Springer-Verlag: Berlin, 1987.
(27) This figure was prepared with MolScript, see: Kraulis, P. T. *J. Appl. Crystallogr.* **1991**, *24*, 946.
(28) Tam, J. P.; Merrifield, R. B. In *The Peptides; Analysis, Synthesis and Biology*; Udenfriend, S., Meienhofer, J., Eds.; Academic Press: New York, 1987; pp 185−244.

MA950703E